

A new shape memory porous material made up of a single entangled NiTi wire

B. Gadot^{a,b}, L. Orgéas^a, D. Rodney^b, S. Rolland du Roscoat^a, D. Bouvard^b

. CNRS, 3SR^(a) and SIMAP^(b) Labs,
Domaine Universitaire, 38400 Saint Martin d'Hères
. Université de Grenoble Alpes, 3SR^(a) and SIMAP^(b) Labs,
Domaine Universitaire, 38400 Saint Martin d'Hères

Mots clefs : Shape Memory Porous Materials ; Self-Entangled Fibrous Structure

1 Introduction

Due to their good biocompatibility and their potentially interesting mechanical properties, porous NiTi materials are promising architected media for biomedical applications. Up to now, most of these materials have been processed *via* powder metallurgy technologies, *e.g.* by consolidating NiTi powders followed by sintering them at rather high temperatures ($\approx 1373\text{K}$). However, the resulting NiTi porous materials exhibits rather poor mechanical properties. This is mainly due to the difficulty (i) of minimising the growth of brittle oxides skins onto the NiTi grains at high temperatures and (ii) of subjecting the NiTi porous materials to relevant thermomechanical treatments after sintering to provide them optimal superelasticity and shape memory effect [1, 2, 3]. Aydogmus *et al.* have recently shown that using magnesium as space holder was a good way to reduce oxide growth during the sintering phase, but the porous structure they produced did not lead to proper superelastic behavior [2, 3].

To circumvent the above difficulties, an original processing route is here proposed to create a NiTi porous material by entangling a single wire in order to provide the porous material with a cohesive behavior. This process does not require the NiTi wire to be sintered at high temperatures, and hence leads to unoxidized material. Besides, it involves various shape setting sequences of the wire with proper thermomechanical treatments at moderate temperatures. Tuning the sequences parameters allows both the microstructure and the shape memory properties of the resulting porous material to be easily tailored. The method used to prepare such an architected shape memory material is presented hereafter, together with its microstructure and the resulting properties of the wire that constitutes it. The macroscale thermomechanical properties of the entanglement is then investigated.

2 Material and Sample Processing

The processing route used to produce the present NiTi porous material is inspired by the method proposed by Tan *et al.* in the case of ductile and elastoplastic Al wires [4]. As sketched in Fig. 1, this method allows homogeneous porous metallic samples to be processed quite easily (i) by progressively entangling plastically deformed wires, from a straight wire to a spring, then from the spring to a spring entanglement, and (ii) by consolidating the entanglement with a close die compaction operation.

Hence, a standard biomedical-grade Ni-50.8at.%Ti in cold worked state with a diameter of $500\ \mu\text{m}$ was chosen for its biocompatibility and for its capability to exhibit good superelastic behaviour and shape memory effect from short and low temperature heat treatments. It was supplied by Forth Wayne Metals. In its initial state, the wire exhibited an elasto-plastic behaviour with a high yield stress ($\approx 1800\ \text{MPa}$) and a rather small ultimate strain of ≈ 0.04 . These features are not in good accordance with the low yield stress and the high ductility required to process the porous material according

to the method proposed by Tan *et al.* Indeed, it is well-known that entangling straight wires with a large elastic domain is not straightforward [5, 6] : (i) it usually yields to very heterogeneous porous materials with uncontrolled and undesirable gradient of porosity and (ii) it requires the entanglement to be confined within a container to avoid huge elastic spring back effects after processing. To overcome these difficulties, the deformed NiTi wire was thus subjected to a short heat treatments of 2 min at 623 K (followed by water quenching) after each shaping operation depicted in Fig. 1, thus allowing an optimal wire placement and minimized spring back effects. The temperature and the duration of the adopted heat treatments were also optimized in order to provide the produced entanglement good superelastic properties at room temperature (*state 1*) [7]. Therefrom, it was also possible to tailor the entanglement properties by subjecting it to additional heat treatments. For example, to shift its superelastic domain to higher temperatures, *i.e.* to provide it a ferroelastic behavior at room temperature and a shape memory upon heating, the entanglement was heated for 1 h at 723 K and water quenched (*state 2*).

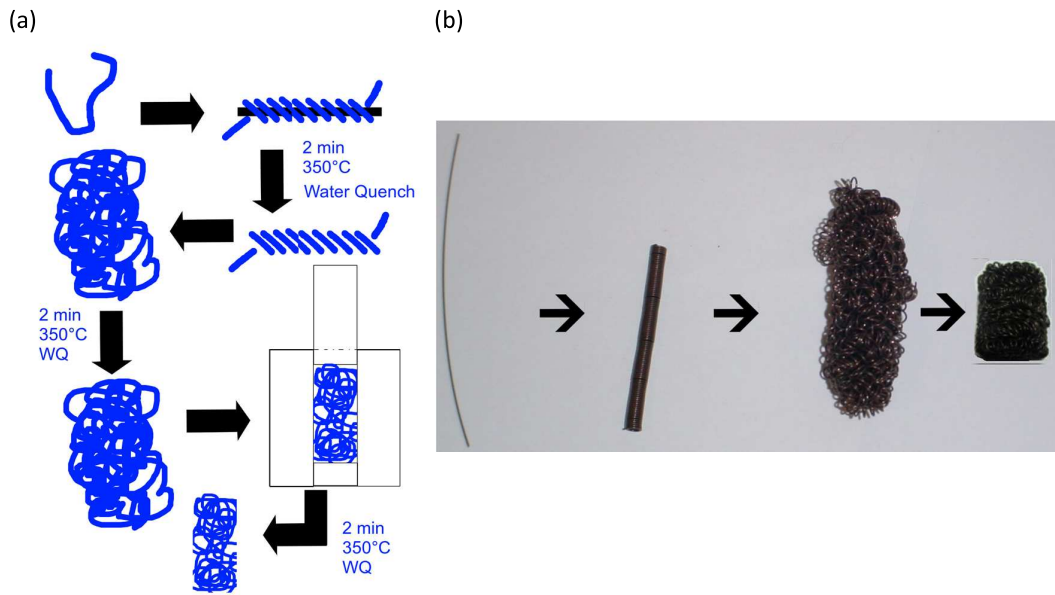


FIGURE 1 – Scheme of the various shape setting operations used to process the NiTi porous material (a) and pictures of the resulting shape settings (b).

3 Wire and Microstructure Characterization

– The free stress forward and reverse transformations of the wire entanglement in *states 1* and *2* were analyzed by cutting small wire pieces inside the entanglement and subjecting them to DSC measurements. Besides, to estimate the wire entanglement mechanical properties, straight wires were subjected to the same thermal history as that followed by the entanglement. Their tensile mechanical behaviour was then assessed at various testing temperatures ranging from 293 K to 353 K and by subjecting the wire to load-unload sequences at a low strain rate of 10^{-3}s^{-1} . The results of these experiments have been gathered in Fig. 2. As shown in Fig. 2(a), DSC measurements recorded for the entanglement in *state 1* emphasise a single transformation peak upon cooling or heating, presumably associated with forward A-M (Austenite to Martensite) and reverse M-A martensitic transformations, respectively. These peaks are very flat and the peak temperature upon heating is close to the room temperature, *i.e.* 293 K. Conversely, in *state 2*, the entanglement exhibited two stages A-R-M (Austenite to R phase to Martensite) and M-R-A transformations respectively upon cooling and heating with pronounced transformation peaks, and the end of these transformations upon heating is close to 328 K. As revealed from Fig. 2(b), the mechanical behaviour of the heat treated wires at room temperature is nicely superelastic in *state 1* whereas it is ferroelastic in *state 2*.

2, the strain induced upon loading (mainly ascribed to stress-induced forward transformation) being weakly recovered upon unloading. Besides, it is worth noting that for both states, transformation stresses recorded at the onset of the forward transformation nicely fit a Clausius-Clapeyron like relation, with a slope close to 5 MPa K^{-1} , *i.e.* in accordance with values commonly observed for heat treated NiTi alloys [8].

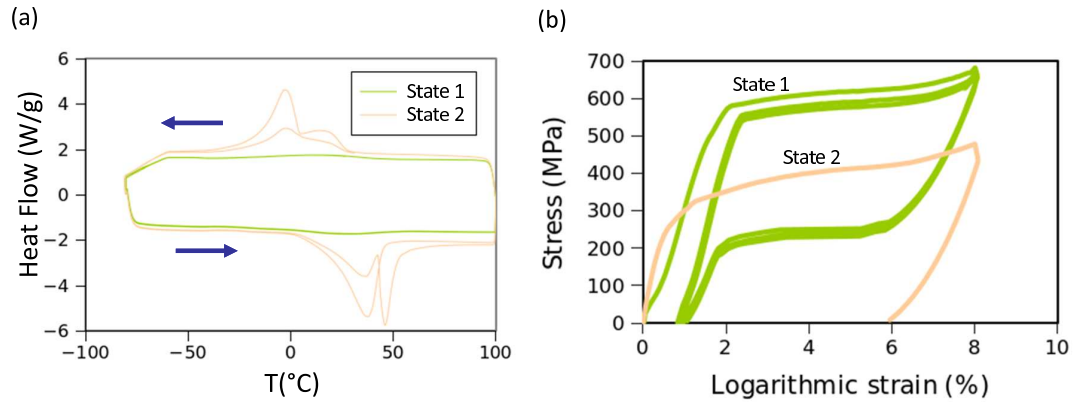


FIGURE 2 – DSC curves (a) and tensile stress-strain curves at room temperature (b) of the treated wire in states 1 and 2.

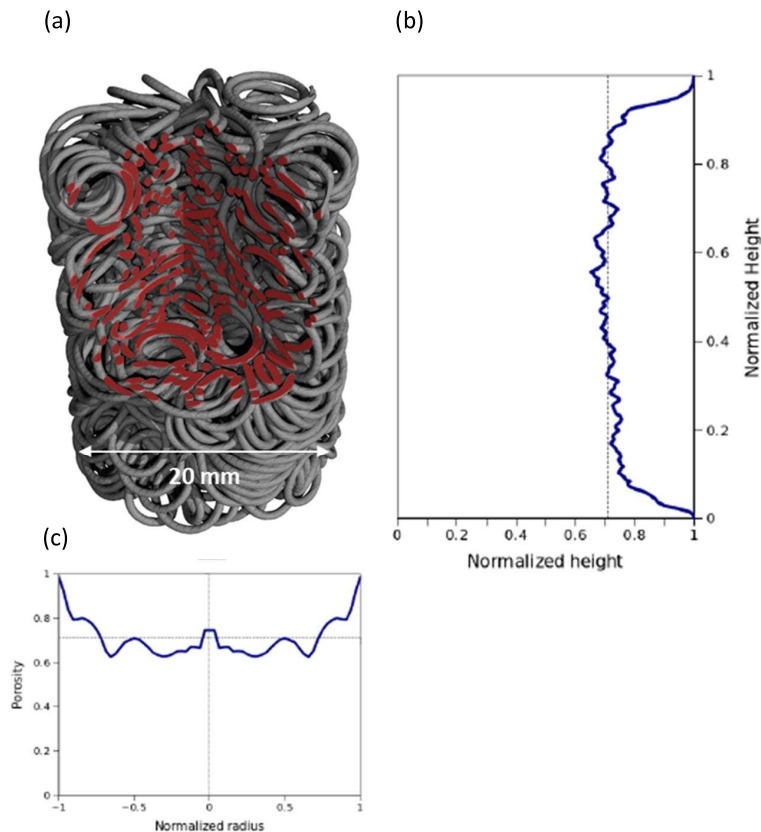


FIGURE 3 – 3D image of the entanglement (a) and corresponding porosity profiles along its height (b) and diameter (c).

- The microstructure of the entanglement in its undeformed state was investigated *via* X-ray microtomography by using a laboratory microtomograph (RX solution, 3SR Lab, Grenoble, France, scans achieved with 1500 X-ray 2D radiographs onto a 1914×1580 pixels CCD detector, voxel size = $7.5 \times 7.5 \times 7.5 \text{ m}^3$). The 3D image shown in Fig. 3 emphasises (i) the nice cylindrical shape of

the produced sample (initial diameter $d_0 = 20$ mm and height $h_0 = 27$ mm) and (ii) its complex two-scale architecture, *i.e.* with a quasi-ordered spring-like pattern that is randomly self-entangled. It is also worth noting that apart from expected small edge effects, the porosity inside the produced sample is fairly homogeneous, with a mean value of ≈ 0.73 (see the porosity profiles reported in Fig. 3).

4 Thermomechanical Properties of the Entanglement

The thermomechanical properties of the processed porous NiTi entanglement was investigated with isothermal uniaxial compression loadings achieved with (i) a compression strain rate of 10^{-3}s^{-1} , (ii) various testing temperatures (from 293 to 353 K) and (iii) various compression strain magnitudes $\varepsilon_a^{max} = \ln(h^{min}/h_0)$ up to -0.3. During the tests, a video camera recorded the deformation of the sample, showing that the compression of the entanglement proceeded with a good macroscale homogeneously, *i.e.* the initial cylindrical sample remained cylindrical in its deformed states. Therewith, it was also possible to estimate its logarithmic radial strain $\varepsilon_r = \ln(d/d_0)$ together with its logarithmic volumetric strain $\varepsilon_v = 2\varepsilon_r + \varepsilon_a$.

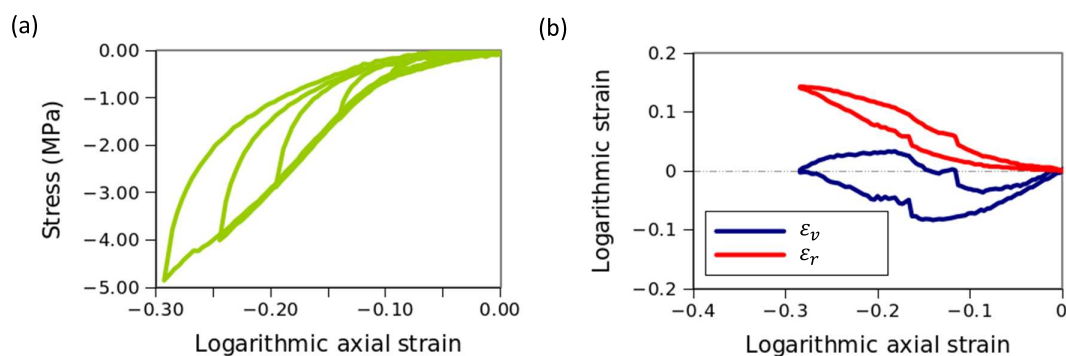


FIGURE 4 – Behavior of the entangled NiTi wire in *state 1* - Uniaxial compression tests at room temperature . Axial stress-strain curves for various maximal axial strain ε_a^{max} (a) and radial and volumetric strains as functions of the axial strain when $\varepsilon_a^{max} = -0.3$ (b).

Fig. 4(a) shows a collection of stress-strain curves recorded during the compression of the entanglement in *state 1* at room temperature. Fig. 4(b) gives the evolution of the radial and the volumetric strains as a function of the axial strain recorded during the compression test with $\varepsilon_a^{max} = -0.3$. Together with the tests achieved with similar testing conditions but at higher temperatures (not shown here), this figure brings up the following comments :

- The shape of stress-strain curves are very different than those usually observed during the compression of other “standard” fibrous materials [9]. Indeed, the compression of fibrous materials usually exhibits a strain hardening that becomes stiffer and stiffer during the compression (here the slope of stress-strain curve first increases but then decreases during loading), the hysteresis observed after the first loading is higher and associated with higher residual strain (here the residual strain is close to zero), cycling the fibrous materials usually conducts to a progressive stabilisation of stress-strain curves (such a stabilisation is not really observed here).
- Whatever the imposed maximal axial strain ε_a^{max} is, the entanglement recovers its initial undeformed state after unloading : it thus exhibits huge superelasticity with moderate hysteresis, up to a compression strain equal to -0.3.
- The hysteretic behaviour of the entanglement is very similar to that observed in the case of bulk Shape Memory Alloys : loops performed with a small strain magnitude always lies within its parent loop, *i.e.* performed at a higher strain magnitude ε_a^{max} [10].
- During the compression, the sample volumetric strain exhibits a complex and amazing behavior. Indeed, during the first stage of the loading, a severe sample consolidation is observed up to an

axial strain $\varepsilon_a = -0.15$, where $\varepsilon_v = -0.08$. Then, a sample dilatancy is recorded so that at the end of the loading, the sample has more or less recovered its initial volume. During the early stage of the unloading, the sample dilatancy is such that the volumetric strain become positive and reaches 0.03. Afterwards, trends observed upon loading are followed with a strain hysteresis. Finally, at the end of the test, the sample volume is fully recovered.

- Tests performed at higher temperature still emphasise a behavior close to that depicted in Fig. 4. Furthermore, it must be pointed out that the temperature dependence of stress levels is close to 0.1 MPa K^{-1} , *i.e.* much lower than the temperature dependency of the transformation stresses of the NiTi wire (see previous subsection).

Although further analysis is certainly required to better understand such an unusual behavior, it seems reasonable to ascribe it to (i) the superelasticity (resp. elasticity) of transformed (resp. untransformed) zones in the wire, (ii) the complex deformation modes of the entangled architected, (iii) dry friction at wire-wire contacts.

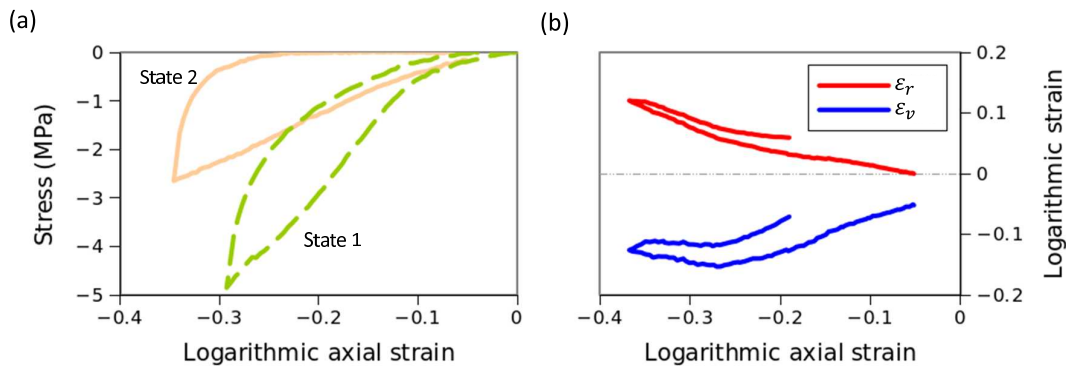


FIGURE 5 – Behavior of the entangled NiTi wire in *state 2* - Uniaxial compression test at room temperature showing the axial stress-strain curve (a) and the radial and volumetric strains as functions of the axial strain (b).

The mechanical behavior of the entangled sample in *state 2* is depicted in Fig. 5. As expected from results plotted in Fig. 2, the superelastic behavior of the sample observed in *state 1* is now replaced by a ferroelastic one, *i.e.* with lower stress levels and with a significant residual axial strain $\varepsilon_a^r = -0.19$. In this case, the volumetric strain ε_v still shows consolidation and dilatancy, but it remains negative and the initial volume is not recovered, *i.e.* a residual consolidation $\varepsilon_v^r = -0.05$ is observed at the end of the test. Once again, this unusual macroscale behaviour may be mainly ascribed to (i) the ferroelasticity (resp. elasticity) of transformed (resp. untransformed) zones in the wire, (ii) the complex deformation modes of the entangled architected, (iii) dry friction at wire-wire contacts.

Lastly, it is important to notice that the large axial and volumetric residual strains induced during the compression of the sample in *state 2* at room temperature can be fully recovered by free-stress heating the sample up to 343 K. Such a huge shape memory effect is illustrated in Fig. 6. Firstly, this figure shows that most of the shape memory recovery occurs between 293 and 328 K, in accordance with the DSC measurements given in Fig. 2. Secondly, the volumetric strain recorded during the shape recovery in *state 2*, *i.e.* during thermal reverse transformation, is positive in between 310 K and 328 K before the sample fully recovers its initial volume, as observed in the case of the superelasticity in *state 1* during stress reverse transformation.

5 Conclusion

Even though the proposed processing route has not yet been optimized to produce perfect superelastic or shape memory porous materials, the first results presented here are very promising. Not only can a cohesive porous material be easily fabricated, but also the behavior can be either superelastic or ferroelastic, depending on the heat treatment achieved during and after the shape setting operations.

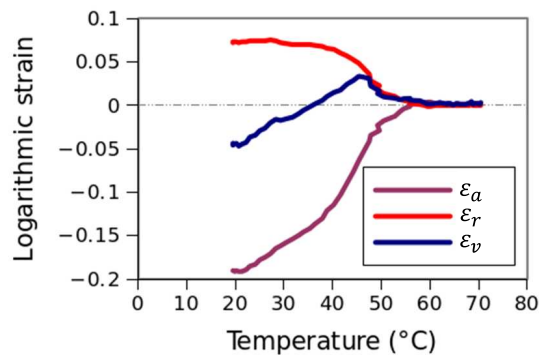


FIGURE 6 – Behavior of the entangled NiTi wire in *state 2* - Shape memory effect showing the evolution of the radial, volumetric and axial strains *vs.* temperature.

Both states have their own interesting properties : in the superelastic state, the material exhibits high stress with up to 30% of recoverable strain. The ferroelastic state shows lower stress, high residual strain and excellent shape memory effect upon heating. For both states, the deformation is homogeneous at the macroscale and the temperature dependence is very low. The entanglement behavior is clearly an interplay between the structure and the material.

Références

- [1] Shearwood, C., Fu, Y.Q., Yu, L., A.Khor, K.. Spark plasma sintering of NiTi nano-powder. *Scripta Mater* 2005 ;52 :455–460.
- [2] Aydogmus, T., Bor, T., BOR, S.. Phase transformation behavior of porous TiNi alloys produced by powder metallurgy using magnesium as a space holder. *Metall Mater Trans A* 2011 ;42A :2547–2555.
- [3] Aydogmus, T., Bor, S.. Superelasticity and compression behavior of porous TiNi alloys produced using mg spacers. *J Mech Behavior Biomed Mater* 2012 ;15(0) :59 – 69.
- [4] Tan, Q., Liu, P., Du, C., Wu, L., He, G.. Mechanical behaviors of quasi-ordered entangled aluminum alloy wire material. *Mater Sci Eng A* 2009 ;527(1-2) :38 – 44.
- [5] Courtois, L., Maire, E., Perez, M., Rodney, D., Bouaziz, O., Bréchet, Y.. Mechanical properties of monofilament entangled materials. *Adv Eng Mater* 2012 ;14 :1128–1133.
- [6] Stoop, N., Wittel, F.K., Herrmann, H.J.. Morphological phases of crumpled wire. *Phys Rev Letters* 2008 ;101 :1–3.
- [7] Pelton, A., DiCello, J., Miyazaki, S.. Optimisation of processing and properties of medical grade Nitinol wire. In : Russell, S., Pelton, A., editors. *Proc of SMST 2000* ; vol. 9(1). 2000, p. 107–118.
- [8] Liu, Y., McCormick, P.. Thermodynamic analysis of the martensitic transformation in NiTi. effect of heat treatment on transformation behaviour. *Acta Metal Mater* 1994 ;42(7) :2401 – 2406.
- [9] Poquillon, D., Viguier, B., Andrieu, E.. Experimental data about mechanical behaviour during compression tests for various matted fibres. *J Mater Sci* 2005 ;40 :5963–5970.
- [10] Orgéas, L., Liu, Y., Favier, D.. Experimental study of mechanical hysteresis of niti during ferroelastic and superelastic deformation. *J Phys IV* 1997 ;C7 :477–82.